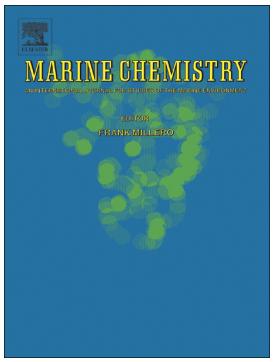

Reconsideration of seawater surfactant activity analysis based on an inter-laboratory comparison study

Philippa C. Rickard, Guenther Uher, Robert C. Upstill-Goddard, Sanja Frka, Nur Ili Hamizah Mustaffa, Hanne Marie Banko-Kubis, Ana Cvitešić Kušan, Blaženka Gašparović, Christian Stolle, Oliver Wurl, Mariana Ribas-Ribas

PII: S0304-4203(18)30200-7
DOI: https://doi.org/10.1016/j.marchem.2018.11.012
Reference: MARCHE 3620

To appear in: *Marine Chemistry*

Received date: 7 August 2018
Revised date: 13 November 2018
Accepted date: 30 November 2018

Please cite this article as: Philippa C. Rickard, Guenther Uher, Robert C. Upstill-Goddard, Sanja Frka, Nur Ili Hamizah Mustaffa, Hanne Marie Banko-Kubis, Ana Cvitešić Kušan, Blaženka Gašparović, Christian Stolle, Oliver Wurl, Mariana Ribas-Ribas , Reconsideration of seawater surfactant activity analysis based on an inter-laboratory comparison study. Marche (2018), https://doi.org/10.1016/j.marchem.2018.11.012

Reconsideration of seawater surfactant activity analysis based on an inter-laboratory comparison study

Philippa C. Rickard[a *], Guenther Uher[a], Robert C. Upstill-Goddard[a], Sanja Frka[b], Nur Ili Hamizah Mustaffa[c], Hanne Marie Banko-Kubis[c], Ana Cvitešić Kušan[b], Blaženka Gašparović[b], Christian Stolle[c,d], Oliver Wurl[c], Mariana Ribas-Ribas[c]

[a]School of Natural and Environmental Sciences, Newcastle University, UK.

[b]Division for Marine and Environmental Research, Ruđer Bošković Institute, Croatia.

[c]Institute for Chemistry and Biology of the Marine Environment, Carl von Ossietzky University of Oldenburg, Germany.

[d]Leibniz Institute for Baltic Sea Research, Warnemünde, Rostock, Germany.

* Corresponding author at: School of Natural and Environmental Sciences, 4th floor, Ridley Building 2, Newcastle University, Newcastle upon Tyne, NE1 7RU, United Kingdom. Email address: p.c.rickard1@newcastle.ac.uk

Abstract

Surfactants, or surface-active substances (SAS), are amphipathic organic substances that adsorb on aquatic phase boundaries, including the air-sea interface that covers ~70% of Earth's surface. SAS thus mediate all mass transfer across the air-sea interface and are central to planetary scale biogeochemical processes. SAS are routinely quantified in seawater and freshwater in terms of total surfactant activity (SA), using alternating current (AC) out-of-phase voltammetry with a hanging mercury drop electrode (HMDE). Although this technique is well established, method modifications have been implemented and differing calibration procedures adopted in individual research laboratories. Increasing interest in the environmental roles of SAS prompts a timely inter-comparison of these varying analytical approaches. Using sea-surface microlayer (SML: uppermost 80 µm layer sampled) and sub-surface (SSW: 1 m depth sampled) seawater from Jade Bay (south-eastern North Sea), we carried out the first inter-laboratory comparison for SA, using methods and calibration protocols previously established in three participating laboratories. Internal calibration protocol follows direct calibrations of individual samples against the model surfactant Triton-X-100 during analysis, whereas external calibration produces independent Triton-X-100 calibration curves; both protocols express SAS concentrations in Triton-X-100 equivalents (T-X-100 eq.). There was no significant difference between SA derived via internal or external calibration protocols, or by using different analytical instruments (range in Kruskall-Wallis and Dunn-Bonferroni post-hoc test p-values: 0.062-1.000), except where freeze/thaw degradation was suspected to have occurred during transit ($p < 0.001$). We recommend using discrete calibration standards during external calibration. Irrespective of any differences in SA determined by the three laboratories, the SA enrichment factor (EF: = SA_{SML}/SA_{SSW}) was not affected for any sample; the root mean square error (± one standard deviation) between all laboratories was 0.156 ± 0. 226 (n = 45). We present and discuss recommendations for a standard analytical protocol to ensure the inter-laboratory compatibility of SAS measurements into the future.

Introduction

Surfactants, or surface-active substances (SAS), are an important subgroup of the organic matter pool in natural waters (Wurl et al., 2009). SAS are a complex mix of molecules that range widely in solubilities, but are all amphipathic; i.e. they possess both hydrophobic and hydrophilic structural groups. SAS include components of the polysaccharide, amino acid, protein, lipid and chromophoric dissolved organic matter (CDOM) pools (Gašparović et al., 1998a; 2007; Kuznetsova et al., 2004; Tilstone et al., 2010; Williams et al., 1986). In seawater, SAS are mostly biologically-derived, arising via phytoplankton release (Gašparović et al., 1998b), during zooplankton grazing (Kujawinski et al., 2002) and from marine bacterial activity (Satpute et al., 2010). SAS concentrations tend to be high in estuarine and coastal waters and to progressively decrease with distance offshore. Generally higher concentrations are detected during the warmer and more productive months (Frka et al., 2009; Pereira et al., 2016), peaking in concert with phytoplankton blooms (Passow, 2002). Additional small contributions derive from terrestrial sources (Pereira et al., 2016), atmospheric volatiles and dust (Peltzer and Gagosian, 1989) and possibly via the in-situ photochemical processing of other dissolved organic molecules (Tilstone et al., 2010).

The amphipathic nature of SAS causes them to accumulate at air-water interfaces. Consequently, they are enriched in the sea-surface microlayer (SML) relative to sub-surface water (SSW) (Frka et al., 2009; Wurl et al., 2009). The SML occupies the uppermost 1000 µm of the ocean (Cunliffe et al., 2013). Physical, chemical and biological processes in the SML, which are distinct from those in the immediately underlying waters (Hardy, 1982), control the rates at which all energy and matter exchange between air and sea, and thus exert short-term and long-term impacts on a range of planetary scale processes, including global biogeochemical cycling, the air-sea exchange of gases and particles, and climate regulation (Cunliffe et al., 2013; Engel et al., 2017). The enrichment of SAS in the SML occurs predominantly via “scavenging” from SSW onto rising bubble surfaces and by diffusion (Wurl et al., 2011). Subsequent bubble bursting and spray entrainment by wind transfer variable amounts of SAS from the SML to the marine boundary layer (Donaldson and George, 2012), where they are a source of organic material to marine aerosols (Leck and Bigg, 1999; Ovadnevaite et al., 2011). Organic compounds with surfactant properties ubiquitously present in atmospheric aerosol particles have the potential to importantly affect the cloud droplet forming ability of these particles (Facchini et al., 1999; Kroflič et al., 2018). In addition, photochemistry in the surface ocean plays important role in marine surfactant film transformation leading to significant abiotic production of unsaturated and functionalized volatile organic compounds (VOCs) acting as precursors for the formation of organic

aerosols (Ciuraru et al., 2015) SAS enrichment of the SML relative to SSW has been found to be ubiquitous, with strong spatiotemporal variability (Sabbaghzadeh et al., 2017; Wurl et al., 2011). The highest SML enrichments in SAS have been seen in low productivity, oligotrophic regions away from terrestrial influences, where SAS concentrations in SSW are generally low (Wurl et al., 2011). This may be explained by proportionately higher bubble scavenging of SAS from oligotrophic SSW (Wurl et al., 2011), reflecting a finite limit to the amount of SAS that can be supplied by any individual bubble to the SML (Sabbaghzadeh et al., 2017).

The solubility of SAS also influences their physical distribution in the SML; calm seas allow insoluble SAS to form visible surface slicks, which have been observed under low to moderate wind stress conditions (Frew et al., 2006), but tend to disperse in wind speeds over ~3-4 m s^{-1} (Liss et al., 1997). In contrast, SML enrichments in soluble SAS have been observed for wind speeds up to 13 m s^{-1} (Sabbaghzadeh et al., 2017) and to be rapidly re-established following strong perturbation (Bock et al., 1999; Frew et al., 1990; Goldman et al., 1988). SML SAS enrichment plays a globally important role by modifying the viscous-elastic properties of the SML, thereby dampening surface turbulence (Hühnerfuss, 2006). The presence of SAS has long been known to suppress the air-sea gas transfer velocity (k_w) of CO_2 and other climate-active gases (Broecker et al., 1978; Downing et al., 1957; Jähne et al., 1987), thereby decreasing their air-sea exchange rates (Upstill-Goddard, 2006). Suppression of k_w by up to 50% is typical, as evidenced by laboratory measurements using natural SAS in seawater (Pereira et al., 2016; 2018) and exudates from phytoplankton cultures (Frew et al., 1990), and by field studies of artificial (oleyl alcohol) SAS slicks (Brockmann et al., 1982; Salter et al., 2011).

Despite the clear importance of SAS at the air-sea interface, expertise in their measurement in natural waters resides in a relatively small number of research laboratories. The total concentration of SAS in a water sample is most commonly quantified as equivalent concentrations of the model surfactant tetra-octylphenolethoxylate (T-X-100, reported in mg l^{-1}), which is expressed as total surfactant activity (SA). Out-of-phase alternating current (AC) voltammetry is an electrochemical method routinely used to quantify SA, which is based on hanging mercury (Hg) drop electrode (HMDE) capacity current (Ic) measurements at a selected potential (-0.6 V, approximately the potential of the electrocapillary maximum) after a defined accumulation period (Ćosović and Vojvodić, 1998). Thus, SAS adsorption at the electrode surface changes the capacity of the electrode double layer. Electrode surface coverage and, indirectly, the decrease in the capacity current relative to a blank electrolyte (ΔIc) for a given accumulation time are functions of SAS concentration in solution (Ćosović et al., 2010). The analysis of SA by AC voltammetry is long-established (e.g. Ćosović and

Vojvodić, 1982; 1998; Kozarac et al., 1976) and increasingly used, but various subsequent modifications of the original method bring into question the comparability of SA measurements. A recent multi-institute study of the SML afforded us the opportunity to directly address this issue, through the first ever direct inter-laboratory comparison of SA measurement techniques, using SML and corresponding SSW samples, collected from Jade Bay, south-eastern North Sea, during April 2017. We report our findings here, along with recommendations for standard analytical protocols for SA determination, which we hope will ensure future consistency among research laboratories quantifying SAS by AC voltammetry. This study will serve as the base for the expansion of SA measurements in other laboratories, which is paramount to progressing our understanding of SAS-mediated biogeochemical processes.

Methods

The SA inter-calibration was carried out during MILAN (sea-surface MIcroLAyer functioning during the Night), a multidisciplinary study of the impact of diurnal changes in solar radiation on SML function. MILAN took place from 3-12 April 2017 in Jade Bay (53° 27' N, 8°12' E), a 190 km^2 coastal inlet of the Wadden Sea in the south-eastern North Sea (Figure 1) (Götschenberg and Kahlfeld, 2008). Inter-calibration partners were the Institute for Chemistry and Biology of the Marine Environment (ICBM), Carl von Ossietzky University of Oldenburg, Germany, The School of Natural and Environmental Sciences, Newcastle University (NU), UK and the Division for Marine and Environmental Research, Ruđer Bošković Institute (RBI), Croatia.

Sample collection and processing

Triplicates of each of a total of 42 Jade Bay water samples were collected from 30 locations selected to provide a range of SA (Figure 1) and assigned to one of four sample "groups". Each participating institute received one of the three replicates. All samples were stored in optically opaque, high density polyethylene (HDPE) sample bottles. The SML (Sample Group 1) and corresponding SSW (Sample Group 2) samples were collected using the remotely operated 4.5 m research catamaran *Sea Surface Scanner* (S^3; Ribas-Ribas et al., 2017) that was deployed from RVs *Otzum* and *Zephyr* during a 25-hour tidal-drift sampling cycle on 8-9 April 2017 (Figure 1). The SML was sampled to a depth ~50–80 µm using a set of six partially immersed rotating glass discs (diameter: 60 cm; thickness: 0.8 cm) bow mounted between the hulls of S^3. SML samples adhering to the disks were automatically directed into a set of sampling bottles by polycarbonate wipers. SSW was simultaneously collected from 1 m depth via a rigid sampling line mounted below S^3. The SML and SSW samples were individually pooled into 20 l carboys, from which subsamples were transferred

in triplicate to the HDPE bottles after 24-48 hours (on 10 April 2017). Samples in Group 3 were collected from easily accessible sources of natural water in and around the ICBM grounds (seawater storage pools; aquarium; nearby harbour) and Sample Group 4 consisted of samples from a ~500-m transect along the nearby beach shoreline (Figure 1). Sample Groups 3 and 4 were collected on 10 April 2017 by hand dipping the HDPE bottles in triplicate to < 20 cm depth at each sampling location. Sample Groups 1-4 were all placed into -20 ºC frozen storage simultaneously on 10 April 2017, within an hour of collection into the HDPE bottles.

SA is routinely determined in unfiltered water (Ćosović, 2005; Gašparović et al., 2007) since the removal of particulate matter by filtration could also remove a significant portion of surfactants (Schneider-Zapp et al., 2013). Additionally, Schneider-Zapp et al. (2013) found that poisoning (with mercuric chloride, silver nitrate or formalin) of riverine and estuarine SML samples prior to storage significantly modified SA, CDOM and fluorescent dissolved organic matter (fDOM), whereas, for most untreated, unfiltered samples stored in the dark at 4ºC, changes in SA over 14 days were not significant. Consequently, all samples in this study were untreated and unfiltered. All samples were stored at -20 ^{0}C because the first available opportunity for simultaneous sample analysis by all participating laboratories was seven weeks after sample collection.

The ICBM replicates remained at -20 ºC at ICBM until concurrent analysis was possible. The NU and RBI replicates were carefully wrapped in freezer packs, transported to the respective laboratories in cool boxes, and placed into -20 ºC storage immediately upon arrival. Cold transit times were ~24 hours (NU) and ~16 hours (RBI). While partial to full thaw was observed for all NU samples on arrival, no significant thawing was evident for the RBI samples.

A defrosting protocol and schedule (Table S.1, supplementary information) was coordinated across the three participating laboratories between 29 May and 2 June 2017; specified samples were defrosted slowly over 24 hours in the dark at 4ºC and analysed the following day. The ICBM analytical protocol limits the sample analysis rate to 3 samples per hour due to the time required to calibrate each sample individually during analysis (see below). This allowed scheduling the analysis of ~10 samples per day.

Analytical protocols

In all three participating laboratories SA analysis followed the method of Ćosović and Vojvodić (1998), using AC out-of-phase voltammetry. All laboratories used the standard three-electrode system, with HMDE working electrodes, Ag/AgCl/3 mol l^{-1} KCl reference

electrodes and platinum coil auxiliary electrodes. ICBM used an automated 747 VA Computrace and NU used an automated 797 VA Computrace (Metrohm, Switzerland: https://www.metrohm.com/en-gb/products-overview/voltammetry/), both with 10 ml sample volumes. RBI analysed 25 ml of duplicate samples on two instruments: 1) RBI1 – a potentiostat/galvanostat µAutolabIII/FRA (Metrohm Autolab B.V., The Netherlands) with a manual Hg drop operation (Polish Academy of Sciences, Poland); and 2) RBI2 – a 663 VA Stand with potentiostat/galvanostat µAutolabII and automated Hg drop production (Metrohm Autolab B.V., The Netherlands). Table 1 summarises specific instrument settings. SA quantification is based on SAS adsorption on the Hg electrode measured by the change in capacity current (ΔIc) at an applied potential (E) of -0.6 V (Ćosović et al., 2010; Ćosović and Vojvodić, 1998), being the approximate value for the electrocapillary maximum and the Hg point of zero charge (pzc) (Avranas and Papadopoulos, 1992; Grahame, 1947).

All three laboratories used glass measurement cells and a 30 s accumulation time (all four instruments) throughout the exercise. All glassware was furnaced at 450 ^{0}C for ≥ 4 hours prior to use, and between samples was acid washed with 10% HCl and rinsed with analytical grade water (18.2 MΩ cm, Milli-Q, Millipore System Inc., USA). When adsorption saturation of the Hg electrode surface occurred within 30 s, samples were diluted with defined volumes of NaCl solutions of known concentration to adjust sample salinities to 0.55 mol l^{-1} NaCl. Calibration was always against the non-ionic soluble surfactant T-X-100 (Sigma-Aldrich, UK; data reported in mg l^{-1} T-X-100 eq.), but the procedures differed in some details between the laboratories.

RBI and NU both employed external calibration as detailed in Ćosović and Vojvodić (1998), in which the capacity current (Ic) for each sample (salinity adjusted to 35 with NaCl) is measured relative to that of a blank electrolyte ($\Delta Ic = Ic_{blank} - Ic_{sample}$). Salinity adjustment assumed salinity 35 ≡ 0.55 mol l^{-1} NaCl and that salinity increases linearly with increasing NaCl concentration:

$$V_2 = V_1 \frac{C_3 - C_1}{C_2 - C_3} \quad (1);$$

$$C_1 = \frac{S_1}{S_2} C_3 \quad (2);$$

where V_1 is the sample volume (ml) in the measurement cell, V_2 is the NaCl volume (ml) required to adjust the sample salinity, C_1 is the NaCl concentration (mol l^{-1}) equivalent to the measured sample salinity (S_1), C_2 is the NaCl concentration (mol l^{-1}) used to adjust sample salinity, C_3 is the NaCl concentration (mol l^{-1}) equivalent to the adjusted sample salinity (S_2).

External calibration with T-X-100, in a NaCl matrix of the same ionic strength as the samples, produces an apparent adsorption isotherm. The linear calibration range (below adsorption saturation) is used to calculate SA at the specified accumulation time (Ćosović, 1990; Ćosović and Vojvodić, 1982; 1998). In calibration, RBI traditionally use discrete T-X-100 calibration standard solutions in the range 0.02-1.30 mg l^{-1}, whereas NU used consecutive T-X-100 standard additions to the blank electrolyte solution (referred to as NU1), obtaining concentrations in the range 0.01-0.75 mg l^{-1} following dilution factor correction. For purposes of inter-comparison, NU therefore followed both protocols in parallel (NU1, and RBI protocol = NU2) to produce two independent calibrations covering the range 0.01-1.35 mg l^{-1} T-X-100 eq. An external calibration protocol comparison was thus included, where SA was quantified from NU raw sample data (ΔI_C values) using both the NU1 and NU2 external calibration curves. NU conducted five potential scans per sample measurement, which produced replicate determinations of I_C at -0.6 V within 1% for the blank electrolyte. Replicate sample response curves were accepted if they visibly overlapped (< 1% difference; Figure S.1, supplementary information). Table 2 summarises the external calibration parameters used by NU and RBI.

ICBM used an internal calibration method following Sander and Henze (1997), where each sample was calibrated individually during analysis (e.g. Figure 2). Here, a blank electrolyte of 0.55 mol l^{-1} NaCl was measured, followed by the sample alone, and with standard additions of T-X-100 to final concentrations of 0.1, 0.2, 0.3 mg l^{-1}; one potential scan was conducted per addition. Three to four replicate aliquot samples were measured, resulting in relative standard deviations below 6%, with SA calculated from a blank electrolyte corrected regression line (SA T-X-100 eq. = intercept (μA) / slope (μA / T-X-100 mg l^{-1}). This results in a reduced matrix effect and precludes a need to adjust the sample salinity (Sander and Henze, 1997; Wurl et al., 2011).

On automated HMDE electrodes, Hg drop production is controlled by compressed N_2 (~1 bar). To ensure stable and uniform size drops for a consistent surface area for surfactant adsorption, stable N_2 pressure is maintained throughout. With the manual HMDE electrode used by RBI, N_2 gas is not required because the Hg drop size is set manually at the start of the analysis using a graduated scale and reproduced by manual operation throughout. The automated and manual instruments both require recalibration if the factors affecting the size of the Hg drop are altered in any way. During analysis, following the extrusion of a few Hg drops, a fresh, stable Hg drop is produced for each measurement. After each analysis the used drop falls to the bottom of the measurement cell; hence a ‘slug’ of waste Hg accumulates until the cell contents are discarded. In the ICBM internal calibration method, this ‘slug’ is discarded at the end of each sample analysis and calibration. During the RBI

(and NU2) external calibration method, waste Hg was discarded following the analysis of each discrete calibration standard. In contrast, Hg waste accumulates during the NU1 method until all the standard additions required to generate an adsorption isotherm are completed.

Data Analysis

The results of the SA analyses for all 42 samples from each of the three participating laboratories were collated and statistically analysed, with the null hypothesis that there were no significant differences between SA values produced by the three participating laboratories, by the different instruments and by the contrasting calibration methods (five datasets in total). Shapiro-Wilk tests (Table S.2, supplementary information) showed the data to be normally distributed for NU1 ($p = 0.212$) and NU2 ($p = 0.227$), but not normally distributed for ICBM, RBI1 and RBI2 ($p < 0.001$ for all). All data were therefore analysed in a consistent way, using non-parametric Kruskall-Wallis and Dunn-Bonferroni post-hoc tests. These were carried out on the whole data set and on the individual Sample Groups (i.e. 1 to 4), for all four instruments and all three calibration protocols. Surfactant Enrichment Factors ($EF = SA_{SML}/SA_{SSW}$) were calculated from the Sample Group 1 (SML) and Sample Group 2 (SSW) data obtained from each dataset and compared.

Results

Figure 3 shows SA (mg l^{-1} T-X-100 eq.) for all samples, instruments and calibration methods and Table 3 gives the median, mean and range of all data, collated and split by Sample Group. Detailed discussion of the spatial and temporal patterns in SA is beyond the scope of this study and will be presented in future publications arising from the MILAN experiment. Nevertheless, all three laboratories identified consistent trends in SA. For Sample Group 1 (SML), SA was highest for SML07 and SML08 and, for Sample Group 2 (SSW), SA was highest for SSW03. For Sample Group 3, results from all participants indicated lowest SA in harbour samples, elevated levels in pool samples, and highest SA values in the aquarium samples. For Sample Group 4 (beach shoreline), all three laboratories found a decrease in SA between Beach01 and Beach02, and a general increase between Beach02 and Beach08. General agreement in overall SA trends among laboratories was therefore apparent although reported SA eq. T-X-100 (mg l^{-1}) showed differences between instruments and calibration methods used.

RBI2 reported the largest range in SA: 0.20-1.51 mg l^{-1} T-X-100 eq. For RBI1 and ICBM, the ranges in SA were similar: 0.05-0.81 and 0.18-1.04 mg l^{-1} T-X-100 eq. respectively. Dunn-Bonferroni post-hoc tests showed no significant difference between the ICBM, RBI1 and RBI2 data sets ($p = 1.000$ for all; Table S.3, supplementary information), hence the null

hypothesis was accepted for these comparisons. The NU2, followed by NU1, data consistently showed the lowest median, mean and range of all laboratories (Table 3). Both the NU1 and NU2 calibration curves were strongly linear (R^2 = 0.99 for both; Table 2), but they showed different slope factors: 7.57 µA/T-X-100 mg l^{-1} for NU1 and 11.24 µA/T-X-100 mg l^{-1} for NU2. Consequently, the range, median and mean in SA determined following the NU1 protocol exceed those obtained via NU2 by factors of 1.28, 1.27 and 1.26 respectively (Table 4). Even so, this difference was not found to be significant (Dunn-Bonferroni, $p = 0.062$). Both NU1 and NU2 datasets were significantly different (lower) to all ICBM, RB1 and RBI2 datasets (Dunn-Bonferroni, $p < 0.001$ for all). Differences in the medians, means and ranges among the three laboratories, for the whole data set and for data split by Sample Group, are summarized in Table 4. The full results of the statistical tests are summarized in the supplementary information (Tables S.2 and S.3).

With the data split by Sample Group, the lowest range for all datasets is Sample Group 2 followed by Sample Group 1 (Table 3). The greatest range for ICBM, NU1 and NU2 was found in Sample Group 3, while for RBI1 and RBI2 it was Sample Group 4. Sample Group 3 was the only group to comprise samples from a range of contrasting sampling locations, and the three participating laboratories diluted these samples to varying degrees. All of Sample Group 3 required dilution at NU; Pool01, Pool02(A-C) and Aquarium(A-C) required dilution at RBI, while no dilution was required for any ICBM Sample Group 3 replicates. Dunn-Bonferroni post-hoc tests showed no significant difference between ICBM, RBI1 and RBI2 with the data split by Sample Group for all comparisons, except for ICBM and RBI2 in Sample Group 2 ($p = 0.012$; Table S.3, supplementary information). Results of comparisons involving the NU1 and NU2 data were not consistent across Samples Groups or laboratory comparisons. No significant difference was found between NU1 and NU2 for Sample Groups 2, 3 and 4. NU1 was not significantly different from ICBM (Sample Group 1), RBI1 (Sample Groups 1, 3 and 4) and RBI2 (Sample Groups 1, 2 and 4). However, NU2 was found to be not significantly different from ICBM (Sample Group 2) only.

SA EFs calculated from Sample Group 1 (SML) and 2 (SSW) data for all laboratories are shown in Table 5. The root mean square error (± one standard deviation) between EF determinations by individual laboratories was 0.156 ± 0. 226 (n=45; Table S.4, supplementary information), showing that EFs largely agreed between laboratories. However, due to all calculated EF values being close to 1.0 there was some disagreement as to whether SML samples were enriched in SA (i.e. EF > 1). NU1 and NU2 both found the same six samples to be enriched; there was little (0.1, Sample 2) to no difference between the NU1 and NU2 EFs which were calculated from datasets produced from the two different calibration curves shown in Table 2. ICBM found five SML samples to be enriched. RBI1

found Sample 8 only to be enriched, whereas RBI2 indicated enrichment in Samples 1 and 7. Samples 5 and 9 were the only samples where EF < 1 for all laboratories, instruments and calibration methods. Mean inter-laboratory EFs indicated SML enrichment in three samples, with the lowest mean EF of 0.9 for all remaining six samples.

Discussion

In this first (to our knowledge) inter-comparison of different SAS analysis methods, no significant differences in SA (Dunn-Bonferroni, $p = 1.000$) were found between two of the three laboratories involved (ICBM and RBI: instruments 1 and 2). These results suggest that comparable results can be produced with automated or manual Hg drop instrumentation, and with internal or external calibration methods. The ICBM internal calibration method allows each sample to be calibrated individually during measurement. This reduces the matrix effect and removes the need to adjust sample salinity (Sander and Henze, 1997; Wurl et al., 2011) but it is more time consuming than the external calibration method. For a 30 s accumulation time, internal calibration allows up to 3 samples per hour to be analysed whereas external calibration allows ~10 samples per hour (including sample salinity adjustments). Additionally, an external calibration is required only once per sample set provided that all instrumental settings (e.g. N_2 pressure, Hg drop size, method parameters etc.) remain constant. An external calibration using discrete calibration standards takes ~3 hours to complete independently of sample analyses (including the preparation of calibration standards). Taken together, SA determinations via external calibration will allow the processing of ~70 samples over a 10-hour period, compared to ~30 samples via internal calibration.

The systematic difference (slope factor difference = 33%) between the two external calibration methods (NU1 and RBI; NU2) translates to borderline evidence of no significant difference (Dunn-Bonferroni, $p = 0.062$) in SA when calculated from the same NU raw ΔI_C data. SA derived using standard additions (NU1) was consistently higher than with the discrete calibration standards (NU2), by a factor of 1.3 for median and mean. This reflects the accumulation of waste Hg in the bottom of the measurement cell during the NU1 calibration procedure, which provides an additional surface for surfactant adsorption that is not available under the NU2 calibration protocol. This additional pathway for T-X-100 adsorption lowers ΔI_C during the NU1 procedure, resulting in elevated SA estimates (Figure S.2, supplementary information). In addition, the NU1 procedure may cause over-stirring, as the convective action over the course of all standard addition measurements is greater than that of each individual calibration standard measurement during RBI protocol (NU2). Stirring accelerates adsorption of T-X-100 from the bulk sample to available interfacial boundaries

(Ćosović, 1990), including Hg surfaces, cell walls and the air-water interface. Ultimately, the experimental conditions for the RBI (NU2) protocol are the same as that of a single sample measurement and result in a more accurate calibration curve than that for NU1, for estimating SA using ΔIc. Notably, SA data produced using these calibrations only minimally affected the EF values derived, the root mean square error (± one standard deviation) being 0.15 ± 0.23 for all data between all laboratories, instruments and calibration methods. Nevertheless, we recommend that for consistency into the future, the RBI (NU2) discrete calibration protocol be followed when using external calibration.

A consistent accumulation time (30 s) throughout this study necessitated some sample dilution. This follows Ćosović and Vojvodić (1998), who advocate sample dilution when SA is high enough to cause saturation of the Hg surface with SAS during sample analysis. The surface area of the Hg drop ultimately dictates when and by how much a sample requires dilution; the smaller the surface area the more rapidly surface saturation will occur. This is evidenced by the difference in surface areas of the Hg drops for the four instruments used (Table 1: ICBM > RBI1 > RBI2 > NU), and the resulting dilutions required for Sample Group 3; NU diluted all samples, RBI diluted three samples and ICBM diluted none. Sample dilution introduces some uncertainty into the data, which reflects the kinetics of SAS adsorption. In the complex mix of SAS in a typical seawater sample, individual compounds compete for adsorption sites on the electrode (Ćosović, 1990). In dilute solutions, the low concentration of strongly adsorbable SAS will displace any initially adsorbed higher concentration of less adsorbable SAS through diffusion (Ćosović, 1990; Fainerman et al., 2010). SAS adsorption at the electrode surface and the resulting change in capacity current (ΔIc) are determined by the specific concentration and properties of the individual SAS in solution (Ćosović, 1990), which could vary with the extent of dilutions. When possible, sample dilution should therefore be avoided, and an alternative accumulation time used (and calibrated for). If dilution is the only option, a series of dilutions should be carried out to ensure linearity over the concentration range of the calibration curve for the specified accumulation time employed. Once the appropriate dilution factor is determined, best practice would be to apply the same dilution factor to all samples of the corresponding sample set.

Caution is also advised when making repeated measurements on the same sample. NU routinely conduct five potential scans on one sample aliquot, where a < 1% difference between Ic at -0.6 V translates to a < 6% difference in calculated SA for undiluted samples. However, using three random samples in this study, RBI detected a 15-20% SAS loss when transferring the same sample solution from one cell (automated; RBI2) to another (manual; RBI1), possibly due to SAS loss on the measurement cell walls and/or Hg drop waste.

Ideally, replicate aliquot samples should be used if numerous measurements necessitate sample transfer, as once analysis is complete samples should not be reprocessed.

Differences in sampling methods between Sample Groups likely contributed some variability to the SA data. Sample Groups 1 and 2 were autonomously collected directly into 20 l carboys at the sampling location and later split by hand into replicate sample bottles, whereas Sample Groups 3 and 4 were collected by hand directly into replicate sample bottles at each sampling location. This methodological difference may be reflected in the fact that the lowest ranges in SA were reported for all laboratories for Sample Groups 1 and 2. Instrument specific factors such as Hg drop surface area, stirring speed, AC voltage frequency and electrochemical cell volumes, have not been accounted for but they could feasibly contribute additional data variability.

SAS concentrations were significantly lower in both NU1 and NU2 (Dunn-Bonferroni, $p < 0.001$ for all) than in ICBM, RBI1 and RBI2. This difference could, at least in part, be explained by differences in sample storage and freeze/thaw degradation. For this inter-comparison study, simultaneous sampling, freezing and pre-measurement thawing protocols were implemented, but transport times for frozen samples differed between laboratories (ICBM, 0-h; NU, ~24-h; RBI, ~16-h). Sample transfer to NU took the longest time, and upon arrival, partial to full thaw of all samples was noted before they were again frozen at -20 °C. Freeze/thaw is not without detrimental effects to SAS components. Schneider-Zapp et al. (2013) found an increase in estuarine SA and CDOM following one -20 °C freeze/thaw cycle of 0.2 µm (surfactant free cellulose acetate) filtered riverine and estuarine water, relative to unfiltered replicates stored at 4 °C for 7, 14 and 28 days. Spencer et al. (2010) found changes in DOC, CDOM and fDOM to be less than ±2% following freeze/thaw of 0.7 µm (GF/F) filtered freshwater samples. For unfiltered freshwater samples, however, Hudson et al. (2009) reported sample specific decreases in the fluorescence intensity over five successive freeze/thaw cycles. Changes during storage cannot be easily predicted and are dictated by initial SAS content and probably the overall sample composition (e.g. CDOM, fDOM; Schneider-Zapp et al., 2013).

It is plausible that the freeze/thaw protocol used in this study may have initiated cell lysis and subsequent SAS release. Intracellular freezing during freeze/thaw is known to cause cellular damage (Lepesteur et al., 1993) and indeed, freeze/thaw is an existing standard protocol used, for example, in the extraction of nucleic acids from bacteria (e.g. Fuhrman et al., 1988) and membrane protein from phytoplankton (e.g. Thoisen et al., 2017). Extraction protocols differ between studies, but typically, cell suspensions are flash frozen in liquid N_2, stored to temperatures as low as -80 °C and most often thawed at ~37°C or above (e.g. Fuhrman et

al., 1988; Lepesteur et al., 1993; Marie et al., 2014; Thoisen et al., 2017; Yuan et al., 2015). However, cell disruption efficiencies are often low (Yuan et al., 2015) and reproducibility can vary. The degree of cell damage depends on the freezing rate; slower freezing allows more water to leave the cells, reduces intracellular ice crystals and has been shown to cause no noticeable cell loss (Lepesteur et al., 1993). In all of these examples freeze/thaw rates and temperatures were more extreme than we used here, and while it is probable that the freeze/thaw cycles in our study caused some cell lysis and SAS release, we contend that any resulting cell damage was likely much less than is reported in these studies. It is also plausible that any SAS release from the NU samples resulting from the first freeze/thaw cycle was masked by SAS degradation during transit and prior to re-freezing. Transit temperatures exceeded that of our controlled laboratory thawing protocol (4°C) and would have resulted in more extensive thawing. At temperatures above 4 °C, enzyme activities are known to increase, with the potential to initiate SAS degradation. In conclusion, we believe it likely that the additional freeze/thaw cycle experienced by the unfiltered NU samples initiated some variable degradation relative to the unfiltered ICBM and RBI samples.

It is common practise to treat natural water samples in preparation for storage prior to analysis. Previous studies have stored filtered natural water samples in the dark at -20 ^{0}C before defrosting overnight prior to the analysis of components such as CDOM, fDOM and dissolved organic carbon (DOC) (e.g. Gao et al., 2010; Spencer et al., 2010). Acidification of filtered DOC samples prior to frozen storage is also routine (e.g. Norman and Thomas, 2014; Tupas et al., 1994). Schneider-Zapp et al. (2013), however, found pre-treatment (e.g. filtration and/or poisoning with formalin, silver nitrate or mercuric chloride) of SML samples to significantly modify SA and CDOM. Within the logistical constraints of this experiment, freezing the unfiltered and untreated samples was the best available storage method to ensure simultaneous analysis of all samples across laboratories and enable comparison of the analytical procedures.

When the split data were statistically analysed by Sample Group, the NU1 data were inconsistently identified as not significantly different from ICBM, RBI1 and RBI2 data (Table S.3, supplementary information). Whereas only one difference with NU2 data was found not to be significant (ICBM, Sample Group 2), notwithstanding the freeze/thaw degradation of NU samples, this was plausibly due to the NU1 method overestimating SA (as discussed above), therefore partly compensating freeze/thaw losses. The ICBM, RBI1 and RBI2 data sets split by Sample Group were not significantly different from each other (Dunn-Bonferroni, $p = 1.000$ for all comparisons), except for ICBM and RBI2 in Sample Group 2 (Dunn-Bonferroni, $p = 0.012$). This overall consistency lends confidence to the comparison of SA data derived via these differing analytical protocols in the literature (e.g. Frka et al., 2009;

Pereira et al., 2016; Sabbaghzadeh et al., 2017; Wurl et al., 2011), provided that sample degradation is minimised by following the storage advice of Schneider-Zapp et al. (2013) and that discrete calibration standards are used in external calibrations. Irrespective of this, the EF values derived in this study are internally consistent and thus evidently are robust. As such, they can be used with some confidence to quantify SAS partitioning into the microlayer and consequently, to evaluate the potential role of SML SAS in global-scale biogeochemical processes (Sabbaghzadeh et al., 2017; Wurl et al., 2011).

Conclusions

We carried out the first inter-laboratory comparison of SAS analysis in replicate seawater samples, using four different instruments, with three different laboratory protocols and calibration methods. The results were not significantly different between laboratories or instruments, except where freeze/thaw degradation is likely to have occurred. Within the logistical constraints of this inter-comparison, freezing the unfiltered and untreated samples was the best available storage method to ensure simultaneous analysis of all samples across laboratories and to allow a valid comparison of methods. For any future work aiming to derive high quality SA data, until a reliable preservation protocol is established, we do not advocate sample storage at -20 °C. Rather, we recommend protocols outlined by Schneider-Zapp et al. (2013): for short-term storage SAS samples should be unfiltered, untreated, kept in the dark at 4 ^{0}C and measured within 24-48 hours of collection. For the accurate quantification of SA in situ, especially in remote locations for which sample transit times may be considerable, real-time field measurements (e.g. Sabbaghzadeh et al., 2017) remain the only realistic option. The operating procedure we advise for SA quantification is that of Ćosović and Vojvodić (1998), using AC out-of-phase voltammetry with a HMDE. Comparable data can be produced by both internal (Sander and Henze, 1997) and external (Ćosović and Vojvodić, 1998) calibration methods. An external calibration is ultimately the most time efficient, but an internal calibration reduces matrix effects; when an external calibration method is used, it should be carried out with discrete calibration standards. Even if SA measurements show some disagreement between studies, our evidence is that EF values will nevertheless be more robust.

Acknowledgements

We could not have carried out this study without the excellent support provided by the Masters and crews of RVs *Senckenberg*, *Otzum* and *Zephyr.* We also thank the staff of ICBM Wilhelmshaven for hosting and for organizational support, and Carl von Ossietzky University, Oldenburg, and Senckenberg Institute, Wilhelmshaven, for providing funding for the MILAN campaign. We highly appreciate the financial support from the project PASSME

to Oliver Wurl, funded by the European Research Council [grant number GA336408], the Carl von Ossietzky University, Oldenburg, and the Senckenberg Institute, Wilhelmshaven. We acknowledge partial financial support from the European Union Seventh Framework Programme [FP7 2007-2013], Marie Curie FP7-PEOPLE-2011-COFUND [GA no291823], through the NEWFELPRO project [Contract no. 47] and a grant from the Croatian Science Foundation under project IP-11-2013-8607. We also thank the Marine biological production, organic aerosol particles and marine clouds: a Process Chain (MarParCloud) project [SAW-2016_TROPOS-2] for providing financial support to Christian Stolle. Finally, we thank the School of Marine Science and Technology, Newcastle University, for funding the Newcastle contribution to this work, Ryan Pereira for his input and support during the initial discussions leading to this study, and Jon Barnes for logistical support vital to the Newcastle contribution.

The following are the supplementary data related to this article.

Figure S.1 Example of five replicate response curves for one analysis (NU blank electrolyte) used in this study. These response curves show a < 1% difference in capacity current (Ic) at the potential (E) -0.6 V, after a 30 s accumulation time.

Figure S.2. Linear calibration curves for the NU1 (standard additions) and NU2 (discrete calibration standards) external calibrations.

Table S.1 Summary of the inter-laboratory schedule for sample collection, freezing, defrosting and analysis for each of Sample Groups 1-4. This schedule was followed simultaneously by all three participating laboratories.

Table S.2 Shapiro-Wilk test for normality of the full datasets, and split by Sample Group, for each of the participating laboratories, instruments and calibration protocols for the complete data set of 42 samples (Sample Groups 1-4) and when split by Sample Group; the test statistic (W), degrees of freedom (df) and probability value (p) are listed for each.

Table S.3 Kruskal-Wallis (K-W) results and Dunn-Bonferroni adjusted p-values between laboratories, calibration protocols and instruments for the complete data set of 42 samples (Sample Groups 1-4) and when split by Sample Group.

Table S.4 Differences from the inter-laboratory enrichment factor (EF) mean. The inter-laboratory and inter-sample variance in EF (± one standard deviation, σ) = 0.024 ± 0.051, and the root mean square error (± one standard deviation, σ) = 0.156 ± 0.226.

References

Avranas, A. and Papadopoulos, N., 1992. Adsorption of surfactants: differential capacitance studies using phase-sensitive alternating current voltammetry. Langmuir, 8(11): 2804-2809.

Bock, E.J., Hara, T., Frew, N.M. and McGillis, W.R., 1999. Relationship between air-sea gas transfer and short wind waves. Journal of Geophysical Research: Oceans, 104(C11): 25821-25831.

Brockmann, U.H., Huhnerfuss, H., Kattner, G., Broecker, H.C. and Hentzschel, G., 1982. Artificial surface films in the sea area near Sylt. Limnology and Oceanography, 27(6): 1050-1058.

Broecker, H.C., Petermann, J. and Siems, W., 1978. The influence of wind on CO2 exchange in a wind-wave tunnel, including the effects of monolayers. Journal of Marine Research, 36: 595-610.

Ciuraru, R. et al., 2015. Unravelling New Processes at Interfaces: Photochemical Isoprene Production at the Sea Surface. Environmental Science and Technology, 49(22): 13199-13205.

Ćosović, B., 1990. Adsorption kinetics of the complex mixture of organic solutes at model and natural phase boundaries. In: W. Stumm (Editor), Aquatic chemical kinetics, Reaction rate of processes in natural waters. Wiley, New York, pp. 291-310.

Ćosović, B., 2005. Surface-Active Properties of the Sea Surface Microlayerand Consequences for Pollution in the Mediterranean Sea. In: A. Saliot (Editor), The Mediterranean Sea. Springer Berlin Heidelberg, Berlin, Heidelberg, pp. 269-296.

Ćosović, B., Kozarac, Z., Frka, S. and Vojvodić, V., 2010. Electrochemical Adsorption Study of Natural Organic Matter in Marine and Freshwater Systems. A Plea for Use of Mercury for Scientific Purposes. Electroanalysis, 22(17-18): 1994-2000.

Ćosović, B. and Vojvodić, V., 1982. The application of ac polarography to the determination of surface-active substances in seawater1. Limnology and Oceanography, 27(2): 361-369.

Ćosović, B. and Vojvodić, V., 1998. Voltammetric Analysis of Surface Active Substances in Natural Seawater. Electroanalysis, 10(6): 429-434.

Cunliffe, M. et al., 2013. Sea surface microlayers: A unified physicochemical and biological perspective of the air–ocean interface. Progress in Oceanography, 109: 104-116.

Donaldson, D.J. and George, C., 2012. Sea-Surface Chemistry and Its Impact on the Marine Boundary Layer. Environmental Science & Technology, 46(19): 10385-10389.

Downing, A.L., Melbourne, K.V. and Bruce, A.M., 1957. The effect of contaminants on the rate of aeration of water. Journal of Applied Chemistry, 7(11): 590-596.

Engel, A. et al., 2017. The Ocean's Vital Skin: Toward an Integrated Understanding of the Sea Surface Microlayer. Frontiers in Marine Science, 4(165).

Facchini, M.C., Mircea, M., Fuzzi, S. and Charlson, R.J., 1999. Cloud albedo enhancement by surface-active organic solutes in growing droplets. Nature, 401: 257.

Fainerman, V.B., Aksenenko, E.V., Petkov, J.T. and Miller, R., 2010. Adsorption Layer Characteristics of Mixed Oxyethylated Surfactant Solutions. The Journal of Physical Chemistry B, 114(13): 4503-4508.

Frew, N.M., Goldman, J.C., Dennett, M.R. and Johnson, A.S., 1990. Impact of phytoplankton-generated surfactants on air-sea gas exchange. Journal of Geophysical Research, 95(C3): 3337.

Frew, N.M., Nelson, R.K. and Johnson, C.G., 2006. Sea slicks: variability in chemical composition and surface elasticity. In: M. Gade, H. Hühnerfuss and G. Korenowski (Editors), Marine Surface Films, Chemical Characteristics, Influence on Air-Sea Interactions and Remote Sensing. Springer, pp. 45–56.

Frka, S., Kozarac, Z. and Ćosović, B., 2009. Characterization and seasonal variations of surface active substances in the natural sea surface micro-layers of the coastal Middle Adriatic stations. Estuarine, Coastal and Shelf Science, 85(4): 555-564.

Fuhrman, J.A., Comeau, D.E., Hagström, Å. and Chan, A.M., 1988. Extraction from Natural Planktonic Microorganisms of DNA Suitable for Molecular Biological Studies. Applied and Environmental Microbiology, 54(6): 1426–1429.

Gao, L., Fan, D., Li, D. and Cai, J., 2010. Fluorescence characteristics of chromophoric dissolved organic matter in shallow water along the Zhejiang coasts, southeast China. Mar Environ Res, 69(3): 187-97.

Gašparović, B., Kozarac, Z., Saliot, A., Ćosović, B. and Möbius, D., 1998a. Physicochemical Characterization of Natural andex-SituReconstructed Sea-Surface Microlayers. Journal of Colloid and Interface Science, 208(1): 191-202.

Gašparović, B., Plavšić, M., Ćosović, B. and Saliot, A., 2007. Organic matter characterization in the sea surface microlayers in the subarctic Norwegian fjords region. Marine Chemistry, 105(1-2): 1-14.

Gašparović, B., Vojvodić, V. and Ćosović, B., 1998b. Excretion of organic matter during an experimental phytoplankton bloom followed using o-nitrophenol as an electrochemical probe. Croatica Chemica Acta, 71(2): 271-284.

Goldman, J.C., Dennett, M.R. and Frew, N.M., 1988. Surfactant effects on air-sea gas exchange under turbulent conditions. Deep Sea Research Part A. Oceanographic Research Papers, 35(12): 1953-1970.

Götschenberg, A. and Kahlfeld, A., 2008. The Jade. Die Küste, 74 ICCE: 263-274.

Grahame, D.C., 1947. The Electrical Double Layer and the Theory of Electrocapillarity. Chemical Reviews, 41(3): 441-501.

Hardy, J.T., 1982. The sea surface microlayer: Biology, chemistry and anthropogenic enrichment. Progress in Oceanography, 11(4): 307-328.

Hudson, N., Baker, A., Reynolds, D.M., Carliell-Marquet, C. and Ward, D., 2009. Changes in freshwater organic matter fluorescence intensity with freezing/thawing and dehydration/rehydration. Journal of Geophysical Research, 114: G00F08.

Hühnerfuss, H., 2006. Basic physicochemical principles of monomolecular sea slicks and crude oil spills. In: M. Gade, H. Hühnerfuss and G. Korenowski (Editors), Marine Surface Films, Chemical Characteristics, Influence on Air-Sea Interactions and Remote Sensing. Springer, pp. 21–36.

Jähne, B. et al., 1987. On the parameters influencing air-water gas exchange. Journal of Geophysical Research: Oceans, 92(C2): 1937-1949.

Kozarac, Z., Ćosović, B. and Branica, M., 1976. Estimation of surfactant activity of polluted seawater by kalousek commutator technique. Journal of Electroanalytical Chemistry and Interfacial Electrochemistry, 68(1): 75-83.

Kroflič, A., Frka, S., Simmel, M., Wex, H. and Grgić, I., 2018. Size-Resolved Surface-Active Substances of Atmospheric Aerosol: Reconsideration of the Impact on Cloud Droplet Formation. Environmental Science & Technology, 52(16): 9179-9187.

Kujawinski, E., Farrington, J. and W Moffett, J., 2002. Evidence for grazing-mediated production of dissolved surface-active material by marine protists. Marine Chemistry, 77: 133-142.

Kuznetsova, M., Lee, C., Aller, J. and Frew, N., 2004. Enrichment of amino acids in the sea surface microlayer at coastal and open ocean sites in the North Atlantic Ocean. Limnology and Oceanography, 49(5): 1605-1619.

Leck, C. and Bigg, E.K., 1999. Aerosol production over remote marine areas-A new route. Geophysical Research Letters, 26(23): 3577-3580.

Lepesteur, M., Martin, J.M. and Fleury, A., 1993. A comparative study of different preservation methods for phytoplankton cell analysis by flow cytometry. Marine Ecology Progress Series, 93: 55-63.

Liss, P.S. et al., 1997. Report Group 1 – Physical processes in the microlayer and the air-sea exchange of trace gases. In: P.S. Liss and R.A. Duce (Editors), The sea surface and global change. Cambridge University Press, Cambridge (UK), pp. 1-34.

Marie, D., Rigaut-Jalabert, F. and Vaulot, D., 2014. An improved protocol for flow cytometry analysis of phytoplankton cultures and natural samples. Cytometry Part A, 85(11): 962-968.

Norman, L. and Thomas, D., 2014. Long-term storage of riverine dissolved organic carbon.

Ovadnevaite, J. et al., 2011. Detecting high contributions of primary organic matter to marine aerosol: A case study. Geophysical Research Letters, 38(2): L02807.

Passow, U., 2002. Transparent exopolymer particles (TEP) in aquatic environments. Progress in Oceanography, 55: 287-333.

Peltzer, E.T. and Gagosian, R.B., 1989. Organic geochemistry of aerosols over the Pacific Ocean. In: R.A. Duce, J.P. Riley and R. Chester (Editors), Chemical Oceanography. Academic Press, London, pp. 281-228.

Pereira, R., Ashton, I., Sabbaghzadeh, B., Shutler, J.D. and Upstill-Goddard, R.C., 2018. Reduced air–sea CO2 exchange in the Atlantic Ocean due to biological surfactants. Nature Geoscience.

Pereira, R., Schneider-Zapp, K. and Upstill-Goddard, R.C., 2016. Surfactant control of gas transfer velocity along an offshore coastal transect: results from a laboratory gas exchange tank. Biogeosciences, 13(13): 3981-3989.

Ribas-Ribas, M., Hamizah Mustaffa, N.I., Rahlff, J., Stolle, C. and Wurl, O., 2017. Sea Surface Scanner (S3): A Catamaran for High-Resolution Measurements of Biogeochemical Properties of the Sea Surface Microlayer. Journal of Atmospheric and Oceanic Technology, 34(7): 1433-1448.

Sabbaghzadeh, B., Upstill-Goddard, R.C., Beale, R., Pereira, R. and Nightingale, P.D., 2017. The Atlantic Ocean surface microlayer from 50°N to 50°S is ubiquitously enriched in surfactants at wind speeds up to 13 m s−1. Geophysical Research Letters, 44(6): 2852-2858.

Salter, M.E. et al., 2011. Impact of an artificial surfactant release on air-sea gas fluxes during Deep Ocean Gas Exchange Experiment II. Journal of Geophysical Research, 116: C11016.

Sander, S. and Henze, G., 1997. AC-voltammetric determination of the total concentration of nonionic and anionic surfactants in aqueous systems. Electroanalysis, 9(3): 243-246.

Satpute, S.K., Banat, I.M., Dhakephalkar, P.K., Banpurkar, A.G. and Chopade, B.A., 2010. Biosurfactants, bioemulsifiers and exopolysaccharides from marine microorganisms. Biotechnology Advances, 28(4): 436-450.

Schneider-Zapp, K., Salter, M.E., Mann, P.J. and Upstill-Goddard, R.C., 2013. Technical Note: Comparison of storage strategies of sea surface microlayer samples. Biogeosciences, 10(7): 4927-4936.

Spencer, R.G.M. et al., 2010. Temporal controls on dissolved organic matter and lignin biogeochemistry in a pristine tropical river, Democratic Republic of Congo. Journal of Geophysical Research, 115: G03013.

Thoisen, C., Hansen, B.W. and Nielsen, S.L., 2017. A simple and fast method for extraction and quantification of cryptophyte phycoerythrin. MethodsX, 4: 209-213.

Tilstone, G.H., Airs, r.L., Vicente, V.M., Widdicombe, C. and Llewellyn, C., 2010. High concentrations of mycosporine-like amino acids and colored dissolved organic matter in the sea surface microlayer off the Iberian Peninsula. Limnology and Oceanography, 55(5): 1835-1850.

Tupas, L.M., Popp, B.N. and Karl, D.M., 1994. Dissolved organic carbon in oligotrophic waters: experiments on sample preservation, storage and analysis. Marine Chemistry, 45(3): 207-216.

Upstill-Goddard, R.C., 2006. Air–sea gas exchange in the coastal zone. Estuarine, Coastal and Shelf Science, 70(3): 388-404.

Williams, P.M. et al., 1986. Chemical and microbiological studies of sea-surface films in the Southern Gulf of California and off the West Coast of Baja California. Marine Chemistry, 19(1): 17-98.

Wurl, O., Miller, L., Röttgers, R. and Vagle, S., 2009. The distribution and fate of surface-active substances in the sea-surface microlayer and water column. Marine Chemistry, 115(1-2): 1-9.

Wurl, O., Wurl, E., Miller, L., Johnson, K. and Vagle, S., 2011. Formation and global distribution of sea-surface microlayers. Biogeosciences, 8(1): 121-135.

Yuan, J., Li, M. and Lin, S., 2015. An Improved DNA Extraction Method for Efficient and Quantitative Recovery of Phytoplankton Diversity in Natural Assemblages. PLOS ONE, 10(7): e0133060.

Table 1 Settings for all four instruments used in the three participating laboratories; all instruments were phase-sensitive in out-of-phase mode and used a hanging mercury drop working electrode (HMDE).

	ICBM	NU	RBI1	RBI2
Hg drop area (cm^2)	0.05600	0.00392	0.01245	0.00520
Stirrer speed (rpm)	2000	1000	2000	3000
Start potential (V)	-0.6	-0.6	-0.6	-0.6
End potential (V)	-0.9	-1.0	-1.85	-1.85
Step potential (V)	-	0.010	0.0201	0.0201
Amplitude (Vrms)	0.01	0.01	0.01	0.01
Modulation time (s)	0.28	0.05	0.21	0.21
Frequency (Hz)	75.00	75.00	77.35	77.35
Phase angle (deg)	90	90	90	90

Table 2 External calibration parameters used in the Newcastle University (NU) and Ruđer Bošković Institute (RBI) laboratories. Calibration variables are the capacity current of the calibration solution measured at -0.6 V relative to the blank electrolyte (ΔIc: μA) and T-X-100 concentration (*TX*: mg l^{-1}).

	NU1	**NU2**	**RBI1**	**RBI2**
R^2	0.9994	0.9940	0.9894	0.9960
Calibration equation	ΔIc = 0.7567*TX*-0.0200	ΔIc = 1.1243*TX*-0.0153	ΔIc = 0.616*TX*+0.0252	ΔIc = 1.9998*TX*+0.0240
Linear Range (*TX*)	0.025-0.648	0.020-0.330	0.020-0.550	0.022-0.280
LOD (*TX*)	0.025	0.020	0.020	0.022

Table 3 Mean (± standard error), median (± standard deviation), minimum, maximum and range for SA (mg l^{-1} T-X-100 eq.), showing SAS concentrations for all data (Sample Groups 1-4) and split by Sample Group, for all laboratories, calibration methods and instruments.

	Mean	± SE	Median	± SD	Min.	Max.	Range
All data (n = 42)							
ICBM	0.367	0.031	0.256	0.202	0.180	1.040	0.860
NU1	0.199	0.008	0.206	0.054	0.082	0.309	0.227
NU2	0.158	0.006	0.162	0.041	0.069	0.246	0.177
RBI1	0.344	0.024	0.290	0.157	0.048	0.813	0.765
RBI2	0.379	0.049	0.293	0.318	0.198	1.508	1.310
Sample Group 1 (n = 13)							
ICBM	0.233	0.018	0.210	0.064	0.183	0.426	0.243
NU1	0.214	0.008	0.207	0.028	0.178	0.270	0.092
NU2	0.167	0.006	0.162	0.021	0.141	0.209	0.068
RBI1	0.232	0.008	0.221	0.029	0.196	0.290	0.094
RBI2	0.222	0.006	0.224	0.023	0.198	0.289	0.091
Sample Group 2 (n = 9)							
ICBM	0.226	0.009	0.234	0.027	0.180	0.261	0.081
NU1	0.220	0.005	0.219	0.016	0.202	0.251	0.049
NU2	0.172	0.004	0.171	0.012	0.158	0.195	0.037
RBI1	0.295	0.008	0.290	0.024	0.271	0.349	0.078
RBI2	0.266	0.008	0.261	0.023	0.239	0.315	0.076
Sample Group 3 (n = 10)							
ICBM	0.401	0.047	0.416	0.147	0.207	0.569	0.362
NU1	0.161	0.020	0.183	0.062	0.082	0.258	0.176
NU2	0.133	0.016	0.153	0.049	0.069	0.208	0.139
RBI1	0.431	0.078	0.389	0.248	0.048	0.813	0.765
RBI2	0.709	0.169	0.422	0.533	0.304	1.508	1.204
Sample Group 4 (n = 10)							
ICBM	0.635	0.056	0.604	0.178	0.417	1.040	0.623
NU1	0.199	0.024	0.162	0.076	0.113	0.309	0.196
NU2	0.159	0.019	0.129	0.061	0.092	0.246	0.154
RBI1	0.445	0.029	0.412	0.092	0.351	0.667	0.316
RBI2	0.354	0.026	0.332	0.082	0.297	0.578	0.281

Table 4 Conversion factors in the mean and median of all data between laboratories, calibration methods and instruments.

	ICBM		NU1		NU2		RBI1	
	Mean	Median	Mean	Median	Mean	Median	Mean	Median
All data (n = 42)								
NU1	1.86	1.24	-	-	-	-	-	-
NU2	2.32	1.58	1.26	1.27	-	-	-	-
RBI1	1.07	0.88	0.58	0.71	0.46	0.56	-	-
RBI2	0.97	0.87	0.52	0.70	0.42	0.55	0.91	0.99

Table 5 Enrichment factors (EFs) calculated from Sample Groups 1 (SML) and 2 (SSW) SA (mg l^{-1} T-X-100 eq.) for each of the three participating laboratories, and the inter-laboratory mean (± one standard deviation). EF ≥ 1 signifies SML SAS enrichment and EF < 1 signifies depletion.

Sample	ICBM	NU1	NU2	RBI1	RBI2	Mean ± σ
1	* 1.3	* 1.1	* 1.1	0.8	* 1.0	1.1 ± 0.2
2	* 1.1	0.8	0.9	0.7	0.8	0.9 ± 0.1
3	* 1.1	* 1.0	* 1.0	0.6	0.7	0.9 ± 0.2
4	* 1.0	* 1.1	* 1.1	0.7	0.8	0.9 ± 0.2
5	0.9	0.9	0.9	0.9	0.8	0.9 ± 0.0
6	0.7	* 1.0	* 1.0	0.9	0.8	0.9 ± 0.1
7	* 1.7	* 1.1	* 1.1	0.7	* 1.1	1.1 ± 0.3
8	0.9	* 1.1	* 1.1	* 1.0	0.9	1.0 ± 0.1
9	0.8	0.9	0.9	0.8	0.9	0.9 ± 0.0

* SML SAS enrichment

Fig. 1. Sampling locations in Jade Bay. Sample Groups 1 (SML) and 2 (SSW) were collected over a 25-hour sampling cycle (8-9 April 2017); the track marked (1, 2) shows the sampling path of the remotely operated research catamaran *Sea Surface Scanner* (*S*^{3}). Sample Group 3 was collected within and around the ICBM grounds (point 3), and Sample Group 4 from the beach shoreline close to ICBM (point 4). Maps were created in Ocean Data View, Schlitzer, R., https://odv.awi.de, 2018.

Fig. 2. Example internal calibration curves for three samples analysed at the Institute for Chemistry and Biology of the Marine Environment (ICBM). One blank corrected calibration curve is produced from each sample analysis. Calibration variables are the capacity current measured at -0.6 V (ΔIc: µA) and T-X-100 concentration (*TX*: mg l^{-1}).

Fig. 3. Concentrations of SAS, expressed as SA (mg l^{-1} T-X-100 eq.), for Sample Groups 1 (SML), 2 (SSW), 3 (in and around ICBM grounds) and 4 (beach shoreline) measured at the Institute for Chemistry and Biology of the Marine Environment (ICBM), Newcastle University (NU) and Ruđer Bošković Institute (RBI). NU applied both NU (NU1) and RBI (NU2) calibration methods. RBI replicate samples were analysed on both a manual (RBI1) and automated (RBI2) potentiostat. Error bars represent standard deviation of replicate measurements. No dilutions were required for Sample Groups 1 and 2, but were required for Sample Group 3: NU (all) and RBI (Pool01, Pool02(A-C), Aquarium(A-C)), and Sample Group 4: RBI (Beach01).

Highlights

- An inter-laboratory quantification of total surfactant activity (SA) in seawater
- Different calibration protocols produced comparable SA measurements
- Discrete calibration standards must be used during external calibration method
- All tested procedures resulted in comparable SA enrichment factors

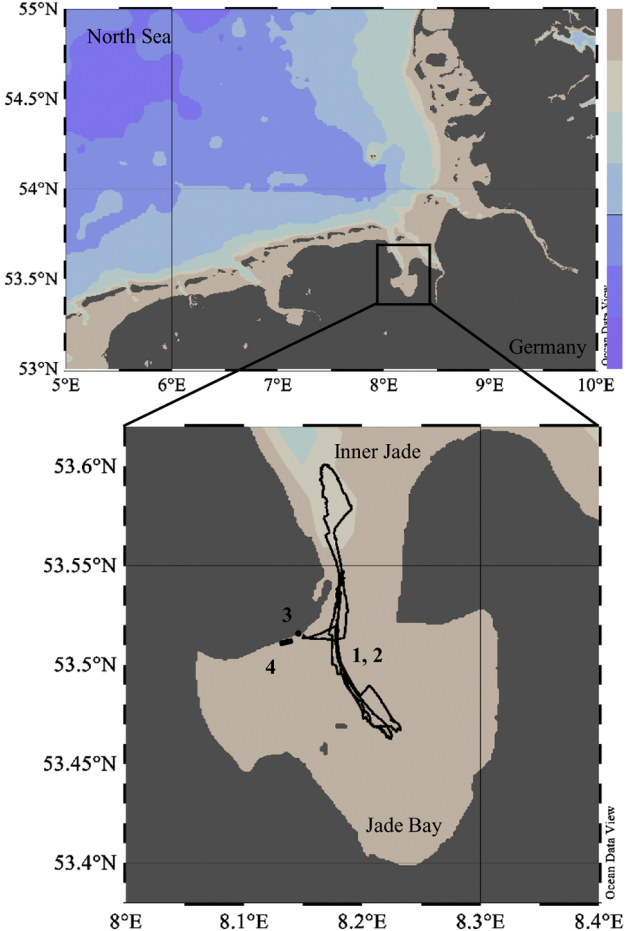
North Sea
Germany
55°N
54.5°N
54°N
53.5°N
53°N
5°E
6°E
7°E
8°E
9°E
10°E
5 m
10 m
20 m
30 m
40 m
50 m
Ocean Data View
Inner Jade
Jade Bay
3
4
1, 2
53.6°N
53.55°N
53.5°N
53.45°N
53.4°N
8°E
8.1°E
8.2°E
8.3°E
8.4°E
Ocean Data View

Figure 1

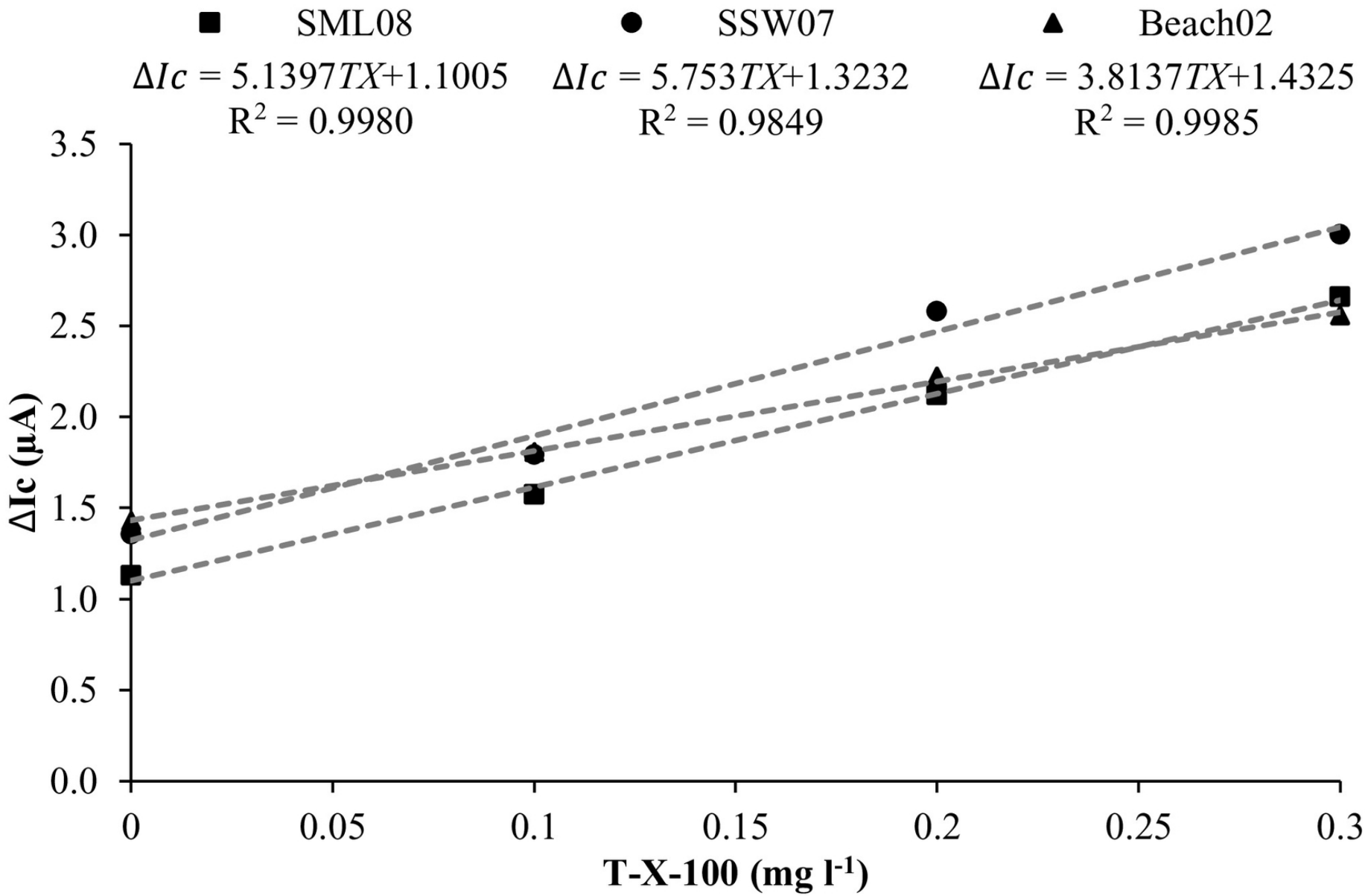
SML08
SSW07
Beach02
$\Delta Ic = 5.1397TX+1.1005$
$R^2 = 0.9980$
$\Delta Ic = 5.753TX+1.3232$
$R^2 = 0.9849$
$\Delta Ic = 3.8137TX+1.4325$
$R^2 = 0.9985$
ΔIc (μA)
T-X-100 (mg l-1)
0.0
0.5
1.0
1.5
2.0
2.5
3.0
3.5
0
0.05
0.1
0.15
0.2
0.25
0.3

Figure 2

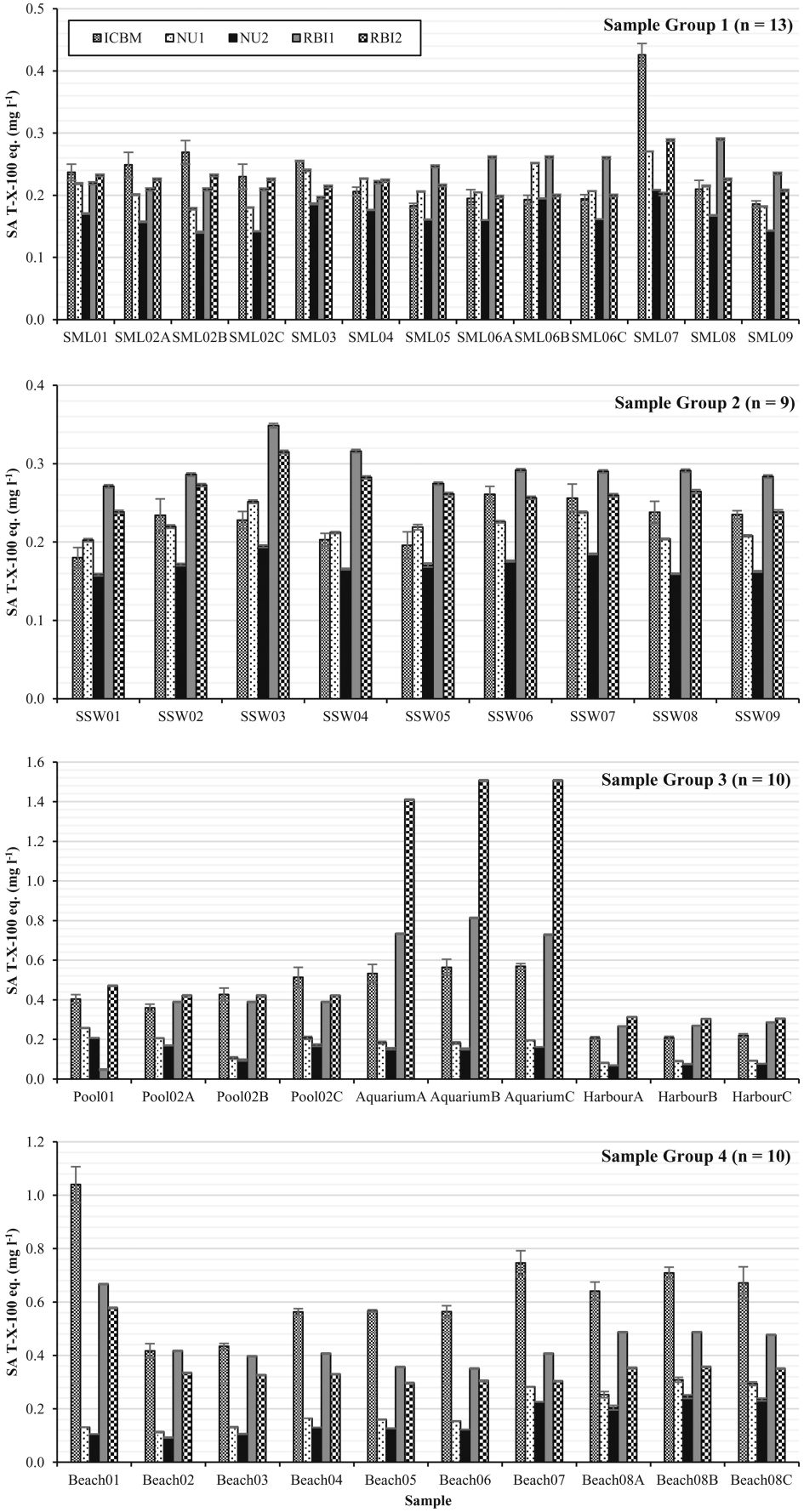
ICBM
NU1
NU2
RBI1
RBI2
Sample Group 1 (n = 13)
SA T-X-100 eq. (mg l-1)
0.0
0.1
0.2
0.3
0.4
0.5
SML01
SML02A
SML02B
SML02C
SML03
SML04
SML05
SML06A
SML06B
SML06C
SML07
SML08
SML09
Sample Group 2 (n = 9)
SA T-X-100 eq. (mg l-1)
0.0
0.1
0.2
0.3
0.4
SSW01
SSW02
SSW03
SSW04
SSW05
SSW06
SSW07
SSW08
SSW09
Sample Group 3 (n = 10)
SA T-X-100 eq. (mg l-1)
0.0
0.2
0.4
0.6
0.8
1.0
1.2
1.4
1.6
Pool01
Pool02A
Pool02B
Pool02C
AquariumA
AquariumB
AquariumC
HarbourA
HarbourB
HarbourC
Sample Group 4 (n = 10)
SA T-X-100 eq. (mg l-1)
0.0
0.2
0.4
0.6
0.8
1.0
1.2
Beach01
Beach02
Beach03
Beach04
Beach05
Beach06
Beach07
Beach08A
Beach08B
Beach08C
Sample

Figure 3